

Conversion of Tungsten(IV) Oxo–Alkyne Complexes to Oxo–Vinylidene Complexes

Todd W. Crane, Peter S. White, and Joseph L. Templeton*

W. R. Kenan, Jr., Laboratory, Department of Chemistry, The University of North Carolina, Chapel Hill, North Carolina 27599-3290

Received December 7, 1998

A series of chiral tungsten(IV) oxo–alkyne complexes of the type $\text{Tp}'\text{W}(\text{O})(\text{I})(\text{RC}\equiv\text{CR}')$ ($\text{R} = \text{R}' = \text{H}$ (**1**); $\text{R} = \text{H}$, $\text{R}' = \text{Me}$ (**2**); $\text{R} = \text{R}' = \text{Me}$ (**3**); $\text{R} = \text{Me}$, $\text{R}' = \text{Ph}$ (**4**); $\text{Tp}' = \text{hydridotris}(3,5\text{-dimethylpyrazolyl})\text{borate}$) has been prepared. These complexes were synthesized by reaction of $\text{Tp}'\text{W}(\text{O})(\text{CO})(\text{I})$ with Me_3NO in the presence of an excess of alkyne. Phenylpropyne complex **4** was isolated as a 2:1 mixture of alkyne rotamers. For the propyne complex, a second route involving deprotonation of acetylene complex **1** followed by addition of MeI also produced complex **2**. The oxidation pathway to **2** with Me_3NO resulted in a 1:1.5 ratio of alkyne rotamers, while the elaboration of **1** via deprotonation/methylation gave **2** in a 9:1 ratio of alkyne rotamers. Addition of $n\text{-BuLi}$ to propyne complex **2** resulted in deprotonation of the terminal acetylene site, and electrophile addition then produced the vinylidene complexes $\text{Tp}'\text{W}(=\text{C}=\text{CMe}_2)(\text{O})(\text{I})$ (**5**) and $\text{Tp}'\text{W}(=\text{C}=\text{C}(\text{Me})(\text{H}))(\text{O})(\text{I})$ (**6**) upon addition of MeI or HCl , respectively. X-ray structure determinations for alkyne complexes **2** and **4** and for vinylidene complex **5** are reported.

Introduction

The stable tungsten(IV) complex $\text{WOCl}_2(\text{CO})(\text{PMePh}_2)_2$ was reported by the Mayer group in 1986.¹ In addition to having the $\text{W}=\text{O}$ fragment, this complex also has the quintessential π -acidic ligand, carbon monoxide, in the coordination sphere. Since then, the Mayer group has developed an extensive array of tungsten(IV) complexes containing both π -acid and π -base ligands.² Other contributions to this field include reports on $\text{Tp}'\text{W}(\text{O})(\text{CO})(\text{I})$,³ $\text{Tp}'\text{W}(\text{O})(\text{S}_2\text{PPh}_2\text{-S})(\text{CO})$, $\text{Tp}'\text{W}(\text{S})(\text{CO})(\text{X})$ ($\text{X} = \text{halide}$)⁴ and the dinuclear species $\text{Tp}'\text{W}(\text{O})_2(\mu\text{-O})\text{W}(\text{O})(\text{CO})\text{Tp}'$.⁵

Despite the electronic contrast between the bonding requirements of oxo and carbonyl ligands, their disparate electronic effects are accommodated in these monomeric d^2 metal complexes. The bonding compromises involved in these π -base/ π -acid complexes have been studied and described.^{2b} In the case of $\text{Tp}'\text{W}(\text{O})(\text{CO})(\text{I})$, donation from the two filled p orbitals of the terminal oxide raises the energy of the d_{xz} and d_{yz} orbitals in forming $\text{M}-\text{O} \pi^*$ molecular orbitals. Back-donation from tungsten to the π^* orbitals of the cis carbonyl ligand

results in lowering the energy of both the d_{yz} and the d_{xy} orbitals. The net result is that the vacant d_{yz} orbital dominates the nonbonding molecular orbital, which reflects the inherent conflict between cis π -donor/ π -acid ligands. Only the CO bonding orbital of d_{xy} parentage among the $d\pi$ orbitals is filled in these stable d^2 complexes (Scheme 1). Detailed calculations comparing cis and trans oxo–carbonyl fragments have also been reported.⁶

Related to this series of π -base/ π -acid compounds are moieties of the type $[\text{M}(\text{O})(\text{RC}\equiv\text{CR})]$.⁷ McDonald and co-workers have synthesized a series of oxotungsten(IV)–alkyne complexes of the type $\text{M}(\text{O})(\text{RC}\equiv\text{CR})(\text{S}_2\text{CNR}_2)_2$ ($\text{M} = \text{Mo}, \text{W}$).⁸ The orientation and electron donation of the coordinated alkynes are readily explained by a three-center–four-electron bonding scheme between the oxo, alkyne, and metal orbitals (*vide infra*).

In other group 6 metal–alkyne chemistry, stereo- and regioselective alkylations of coordinated alkynes have been accomplished.⁹ Intramolecular elaborations have led to the formation of cycloalkynes of the type $\text{Tp}'\text{W}[\text{PhC}\equiv\text{C}(\text{cyclopentyl})](\text{CO})(\text{I})$, $\text{Tp}'\text{W}(\text{cyclooctyne})(\text{CO})(\text{I})$, and $\text{Tp}'\text{W}(\text{cyclodecyne})(\text{CO})(\text{I})$.¹⁰ The cyclooctyne and cyclodecyne complexes were formed by cyclization of the

(1) Su, F.-M.; Cooper, C.; Geib, S. J.; Rheingold, A. L.; Mayer, J. M. *J. Am. Chem. Soc.* **1986**, *108*, 3545.

(2) (a) Bryan, J. C.; Geib, S. J.; Rheingold, A. L.; Mayer, J. M. *J. Am. Chem. Soc.* **1987**, *109*, 2826. (b) Su, F.-M.; Bryan, J. C.; Jang, S.; Mayer, J. M. *Polyhedron* **1989**, *8*, 1261. (c) Bryan, J. C.; Mayer, J. M. *J. Am. Chem. Soc.* **1990**, *112*, 2298. (d) Atagi, L. M.; Over, D. E.; McAlister, D. R.; Mayer, J. M. *J. Am. Chem. Soc.* **1991**, *113*, 870. (e) Atagi, L. M.; Critchlow, S. C.; Mayer, J. M. *J. Am. Chem. Soc.* **1992**, *114*, 1483. (f) Hall, K. A.; Mayer, J. M. *J. Am. Chem. Soc.* **1992**, *114*, 10402.

(3) Feng, S. G.; Luan, L.; White, P.; Brookhart, M. S.; Templeton, J. L.; Young, C. G. *Inorg. Chem.* **1991**, *30*, 2584.

(4) Thomas, S.; Tiekink, E. R. T.; Young, C. G. *Organometallics* **1996**, *15*, 2428.

(5) Young, C. G.; Gable, R. W.; Mackay, M. F. *Inorg. Chem.* **1990**, *29*, 1777.

(6) Brower, D. C.; Templeton, J. L.; Mingos, D. M. P. *J. Am. Chem. Soc.* **1987**, *109*, 5203.

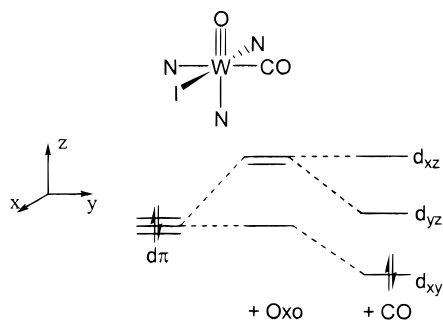
(7) (a) Bokiy, N. G.; Gatilov, Y. V.; Struchkov, Y. T.; Ustynyuk, N. A. *J. Organomet. Chem.* **1973**, *54*, 213. (b) Howard, J. A. K.; Stansfield, R. F. D.; Woodward, P. *J. Chem. Soc., Dalton Trans.* **1976**, 246. (c) Maatta, E. A.; Wentworth, R. A. D. *Inorg. Chem.* **1979**, *18*, 524.

(8) (a) Maatta, E. A.; Wentworth, R. A. D.; Newton, W. E.; McDonald, J. W.; Watt, G. D. *J. Am. Chem. Soc.* **1978**, *100*, 1320. (b) Newton, W. E.; McDonald, J. W.; Corbin, J. L.; Richard, L.; Weiss, R. *Inorg. Chem.* **1980**, *19*, 1997. (c) Templeton, J. L.; Ward, B. C.; Chen, G. J.-J.; McDonald, J. W.; Newton, W. E. *Inorg. Chem.* **1981**, *20*, 1248.

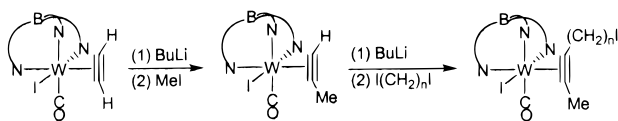
(9) Collins, M. A.; Feng, S. G.; White, P. S.; Templeton, J. L. *J. Am. Chem. Soc.* **1992**, *114*, 3771.

(10) Wells, M. B.; White, P. S.; Templeton, J. L. *Organometallics* **1997**, *16*, 1857.

Scheme 1



Scheme 2



appropriate acyclic precursors, which were formed by elaboration of terminal acetylene compounds (Scheme 2). The parent acetylene complex resists isomerization to the corresponding vinylidene, a reaction observed for many terminal alkyne complexes of d^6 and d^4 metals.¹¹ Additionally, the deprotonated η^2 -acetylide complexes that are proposed as intermediates during elaboration are unusual complexes. To date, no examples of monomeric η^2 -acetylide complexes have been isolated or observed by NMR. However, the analogous η^2 -acetonitrile complex $\text{Tp}'\text{W}(\eta^2\text{-N}\equiv\text{CMe})(\text{CO})(\text{I})$,¹² other side-bound nitrile species,¹³ and η^2 -phosphaalkyne complexes¹⁴ have been isolated.

In this paper, we report the synthesis and structure of a series of tungsten(IV) oxo-alkyne complexes containing the facially coordinating Tp' ligand. Regioselective elaboration of a parent acetylene complex, alkyne rotational behavior, and the formation and structure of d^2 vinylidene complexes are also described. Comparisons to related d^4 metal-alkyne systems are also considered.

Results and Discussion

Synthesis and Characterization of $\text{Tp}'\text{W}(\text{O})(\text{MeC}\equiv\text{CMe})(\text{I})$ (3) and $\text{Tp}'\text{W}(\text{O})(\text{PhC}\equiv\text{CMe})(\text{I})$ (4). The alkyne complexes $\text{Tp}'\text{W}(\text{O})(\text{I})(\text{PhC}\equiv\text{CMe})$ (4) and $\text{Tp}'\text{W}(\text{O})(\text{I})(\text{MeC}\equiv\text{CMe})$ (3) were synthesized by reaction of $\text{Tp}'\text{W}(\text{O})(\text{CO})(\text{I})$ and Me_3NO in the presence of excess

(11) (a) Bruce, M. I. *Chem. Rev.* **1991**, *91*, 197. (b) Nickias, P. N.; Selegue, J. P.; Young, B. A. *Organometallics* **1988**, *7*, 2248. (c) Werner, H. *Angew. Chem., Int. Ed. Engl.* **1990**, *29*, 1077. (d) Lompfrey, J. R.; Selegue, J. P. *J. Am. Chem. Soc.* **1992**, *114*, 5518. (e) Wakatsuki, Y.; Koga, N.; Werner, H.; Morokuma, K. *J. Am. Chem. Soc.* **1997**, *119*, 360. (f) Stegmann, R.; Frenking, G. *Organometallics* **1998**, *17*, 2089.

(12) Thomas, S.; Young, C. G.; Tiekink, E. R. T. *Organometallics* **1998**, *17*, 182.

(13) (a) Wright, T. C.; Wilkinson, G.; Motevalli, M.; Horsthouse, M. B. *J. Chem. Soc., Dalton Trans.* **1986**, 2017. (b) Green, M. L. H.; Hughes, A. K.; Mountford, P. *J. Chem. Soc., Dalton Trans.* **1991**, 1407. (c) Barrera, J.; Sabat, M.; Harman, W. D. *Organometallics* **1993**, *12*, 4381. (d) Kiplinger, J. L.; Arif, A. M.; Richmond, T. G. *Organometallics* **1997**, *16*, 246.

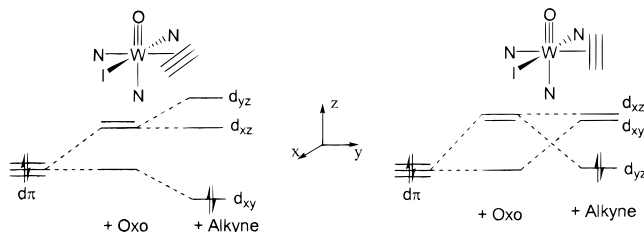
(14) Brauers, G.; Green, M.; Jones, C.; Nixon, J. F. *J. Chem. Soc., Chem. Commun.* **1995**, 1125.

(15) (a) Shvo, Y.; Hazum, E. *J. Chem. Soc., Chem. Commun.* **1974**, 336. (b) Elzinger, J.; Hogeveen, H. *J. Chem. Soc., Chem. Commun.* **1977**, 705. (c) Pearson, A. J.; Shively, R., Jr. *J. Organometallics* **1994**, *13*, 578.

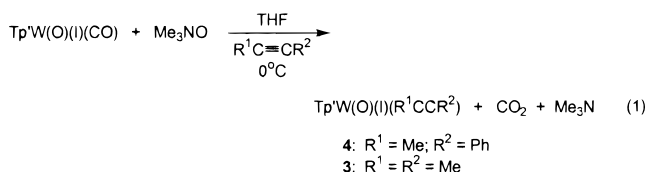
(16) Feng, S. G.; Phillipp, C. C.; Gamble, A. S.; White, P. S.; Templeton, J. L. *Organometallics* **1991**, *10*, 3504.

(17) Templeton, J. L. *Adv. Organomet. Chem.* **1989**, *29*, 1.

Scheme 3



alkyne in THF at 0 °C, with CO_2 as the likely byproduct of oxygen atom transfer to carbon monoxide (eq 1).¹⁵

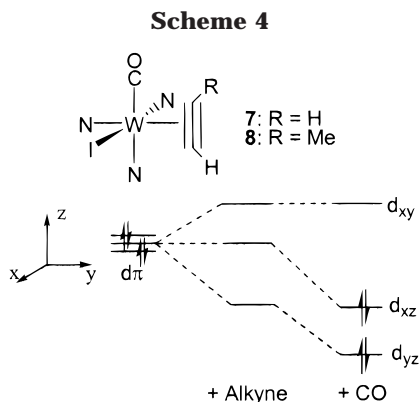


Both complexes were purified by alumina chromatography. Recrystallization from CH_2Cl_2 /pentanes gave an air-stable yellow powder for complex 3, while 4 was isolated as yellow crystals.

The proton NMR spectrum for 4 showed two isomers, which were deduced to be related by alkyne rotation, in a 2:1 ratio at room temperature. The alkyne carbons resonate at 175 and 159 ppm for the major isomer and at 170 and 166 ppm for the minor isomer in the $^{13}\text{C}\{-^1\text{H}\}$ NMR spectrum. Each alkyne carbon has tungsten satellites showing one-bond coupling to tungsten of 30 Hz (^{183}W , 14% abundance). Recrystallization of 4 produced a mixture of crystals further enriched (5:1 by ^1H NMR) in the major alkyne rotamer. The major alkyne rotamer likely has the alkyne phenyl group aligned near the Tp' pyrazole rings due to π -stacking affects observed for other $\text{Tp}'\text{W}(\text{alkyne})$ systems.^{9,16} The ^1H NMR spectrum of butyne complex 3 displays quartets due to a small $^5J_{\text{HH}}$ value of 2 Hz at 3.62 and 2.15 ppm for the distinct alkyne methyl groups. The alkyne carbons of 3 resonate at 167 and 158 ppm, each having one-bond coupling to tungsten of 30 Hz.

The ^{13}C chemical shifts for the alkyne carbons of both 3 and 4 are in the range (140–190 ppm) associated with a three-electron-donor formalism for alkynes.¹⁷ The bonding interactions that result in related three-center molecular orbital electron counting formalisms are well understood.^{8c} Here donation from one oxygen p orbital into a metal d orbital forms a two-center–two-electron bond. Competition between the second filled oxygen p orbital and the filled alkyne π_{\perp} orbital for the same vacant metal $d\pi$ orbital produces a three-center–four-electron bond. The metal–alkyne bonding is completed by back-donation from a filled metal $d\pi$ orbital to the vacant alkyne π_{\parallel}^* orbital. Scheme 3 shows how these bonding interactions are optimal for these d^2 complexes when the alkyne is aligned perpendicular to the metal–oxo axis (for X-ray structures, *vide infra*). In contrast, for d^4 complexes such as $\text{Tp}'\text{W}^{\text{II}}(\text{CO})(\text{alkyne})\text{I}$, which lack the π -base/alkyne three-center–four-electron bonding scheme, the alkyne ^{13}C chemical shifts fall between 200 and 215 ppm and alkyne alignment is along the metal–carbonyl axis.^{9,16}

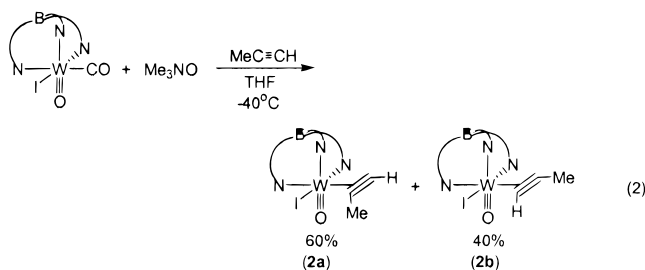
Synthesis and Characterization of $\text{Tp}'\text{W}(\text{O})(\text{HC}\equiv\text{CH})(\text{I})$ (1) and $\text{Tp}'\text{W}(\text{O})(\text{CH}_3\text{C}\equiv\text{CH})(\text{I})$ (2a,b). Addi-



tion of Me_3NO to a THF solution of $\text{Tp}'\text{W}(\text{O})(\text{CO})(\text{I})$ saturated with $\text{HC}\equiv\text{CH}$ produced a brown-red solution containing crude **1**. Purification by alumina chromatography gave **1** as a clean yellow powder in about 60% yield. The acetylene protons resonate at 11.82 and 10.49 ppm in the ^1H NMR spectrum with satellites due to two-bond coupling to tungsten of 13 Hz. The ^{13}C NMR spectrum has resonances at 156 and 145 ppm, each with $^1J_{\text{WC}}$ of 30 Hz, for the acetylene carbons, again reflecting the three-center–four-electron bonding scheme among the oxo, alkyne, and metal.

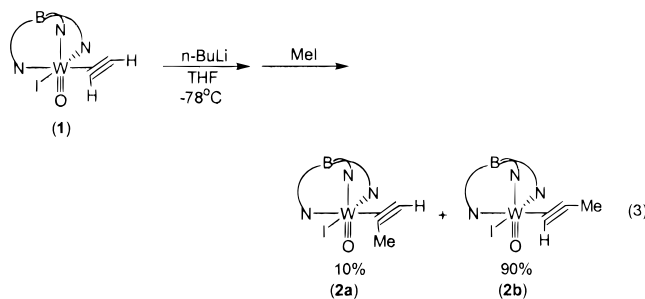
High-temperature ^1H NMR of **1** showed no discernible broadening of the acetylene protons up to 160 °C in $\text{DMSO}-d_6$. The complex also showed no signs of degradation at elevated temperature. Therefore, the barrier for alkyne rotation can be estimated to have a lower limit of 25 kcal/mol. This activation hurdle is higher than the barrier of 19 kcal/mol determined for the tungsten(II) d^4 complex $\text{Tp}'\text{W}(\text{CO})(\text{HC}\equiv\text{CH})(\text{I})$ (**7**).¹⁰ Additionally, the related $\text{W}(\text{O})(\text{HC}\equiv\text{CH})(\text{S}_2\text{CNR}_2)_2$ complex displayed fluxional behavior, but the dynamic process was attributed to dechelation rather than acetylene rotation.^{8c} The preferred alkyne orientation for **7** and the related propyne complex, **8**, is shown in Scheme 4. Note that the parallel orientation of the alkyne and the carbonyl ligands of **7** and **8** can be related to the favored orientation of **1** by a 90° rotation of the alkyne. The high rotational barrier estimated for **1** reflects the specific and strong interactions of the π -basic oxo fragment and the amphoteric alkyne ligand in this d^2 monomer.

Two distinct synthetic routes have been utilized to prepare the propyne complex **2**. The first is analogous to the syntheses of the other alkynes reported here. Approximately 1.5 mL of $\text{CH}_3\text{C}\equiv\text{CH}$ was condensed at low temperature and cannulated into a THF solution of $\text{Tp}'\text{W}(\text{O})(\text{CO})(\text{I})$ at -78 °C. Addition of Me_3NO gave a brown-red solution of crude **2**. With a 20/80 CH_2Cl_2 /hexanes mixture as the eluant, separation of the two isomers differing in alkyne orientation was achieved using an alumina column. An isomer ratio of 1:1.5 was determined by ^1H NMR (eq 2). The major isomer, **2a**, is thought to have the methyl group of the alkyne directed toward the iodide ligand and displays a quartet at 10.54 ($^4J_{\text{HH}} = 2$ Hz) for the terminal alkyne proton which is coupled to the alkyne methyl signal at 3.79 ppm. This assignment is based on comparisons to the related $\text{Tp}'\text{W}(\text{CO})(\text{I})(\text{HC}\equiv\text{CMe})$ (**8**) system. The alkyne methyl group in **8** resonates at 3.6 ppm in the ^1H NMR, a value typical for an alkyne methyl group aligned anti to the



pyrazole rings of Tp' .^{9,10,16} Alkyne methyl groups aligned syn to Tp' resonate about 1 ppm further upfield. Assuming that the alkyne methyl group of **2** behaves in a similar fashion, the methyl resonance at 3.79 ppm is assigned to isomer **2a**. In the ^{13}C NMR, the terminal alkyne carbon is found at 147.2 ppm, while the other alkyne carbon appears at 167.9 ppm. Once again, both alkyne carbons display one-bond coupling to tungsten of 30 Hz.

The second route to **2** involved elaboration of the parent acetylene complex **1**. Addition of a small excess of $n\text{BuLi}$ to a yellow THF solution of **1** at -78 °C resulted in an immediate color change to give a dark purple solution. After the mixture was stirred for 5 min, an excess of MeI was added and this solution was warmed to room temperature. Analytically pure product was obtained by alumina chromatography, which resulted in a 9:1 ratio of **2b** to **2a** (eq 3). Recrystallization from



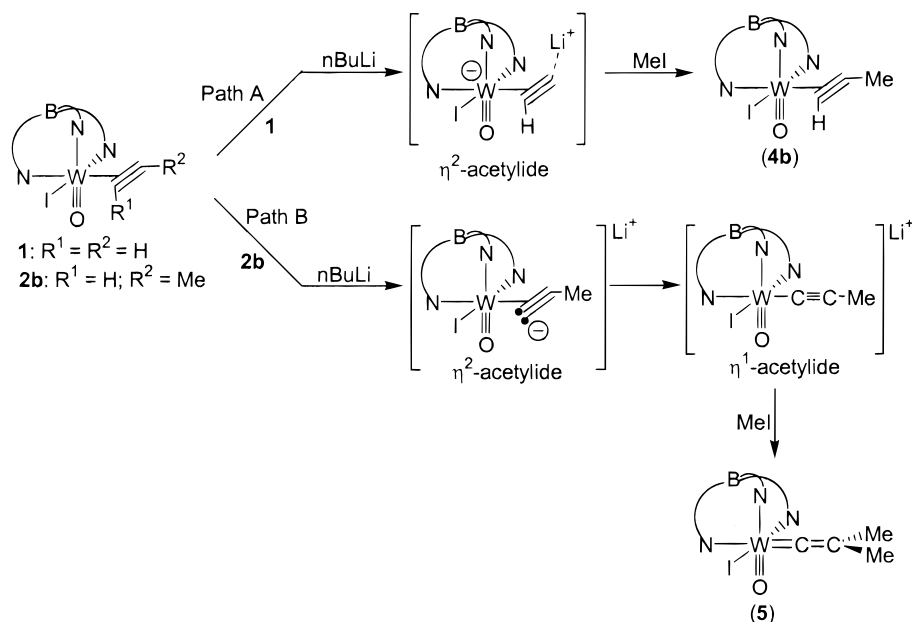
CH_2Cl_2 and pentanes gave X-ray-quality crystals of **2b** containing no detectable trace of isomer **2a**, as assessed by ^1H NMR (vide infra).

Complex **2b** is characterized by a quartet at 11.76 coupled to a doublet at 2.29 ppm ($^4J_{\text{HH}} = 2$ Hz) for the acetylene proton and the alkyne methyl group, respectively. Note the upfield shift of over 1 ppm for the alkyne methyl of **2b** compared to the alkyne methyl of **2a**. Additionally, the difference of over 1 ppm in chemical shift for the terminal alkyne proton between **2a** and **2b** is likely due to the ring current of one of the Tp' pyrazolyl rings and does not denote any difference in acidity. The alkyne carbons are found at 154.9 ppm for the terminal carbon and 154.6 ppm for the carbon bound to the methyl substituent.

The formation of a propyne complex following a deprotonation/methylation sequence with **1** may indicate that formation of an η^2 -acetylide occurs at an intermediate step upon deprotonation (Scheme 5, path A). Presumably, isomerization to an η^1 -acetylide would lead to vinylidene products upon addition of an electrophile (path B, *vide infra*).¹⁸ Given the 9:1 selectivity for

(18) (a) Bruce, M. I.; Swincer, A. G. *Adv. Organomet. Chem.* **1983**, 22, 59. (b) Kostic, N. M.; Fenske, R. F. *Organometallics* **1982**, 1, 974.

Scheme 5



the formation of **2b** vs **2a**, and considering the high barrier for alkyne rotation in **1**, it may be that the sterically demanding iodide ligand controls the site of kinetic deprotonation and causes methylation syn to a Tp' pyrazolyl ring.

X-ray Structures of Tp'W(O)(CH₃C≡CH)(I) (2b) and Tp'W(O)(PhC≡CMe)(I) (4). ORTEP diagrams of **2b** and the major isomer of **4** are shown in Figures 1 and 2. Selected bond distances and angles are given in Tables 1 and 2. The W–N bond lengths of 2.350(5), 2.244(5), and 2.161(5) Å for **2b** and 2.346(3), 2.244(3), and 2.187(3) Å for **4** reflect the decreasing trans influence of oxo, alkyne, and iodide ligands, respectively. The W=O bond distances in **2b** and **4** are nearly identical: 1.712(4) Å for **2b** and 1.710(3) Å for **4**. In addition, the average W–C bond distances are 2.098 Å for **4** and 2.101 Å for **2b**. The preference for the alkyne to align along the W–I axis is evident in each structure.

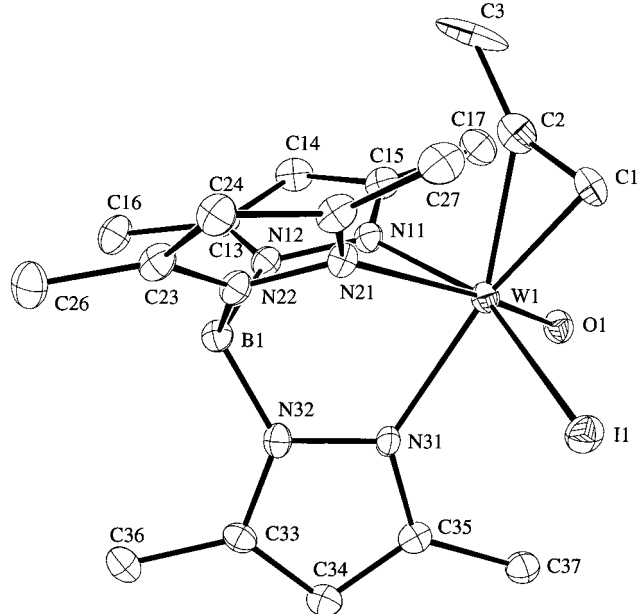


Figure 1. ORTEP diagram for Tp'W(O)(CH₃C≡CH)(I) (**2b**).

Tp'W(=C=CMe₂)(O)(I) (5) and Tp'W[=C=C(Me)-H](O)(I) (6). On the basis of the observed conversion of **1** to **2** via deprotonation/methylation, formation of the 2-butyne complex **3** was expected following deprotonation/methylation of propyne **2**. Indeed, eight methyl signals were observed in the ¹H NMR spectrum of the

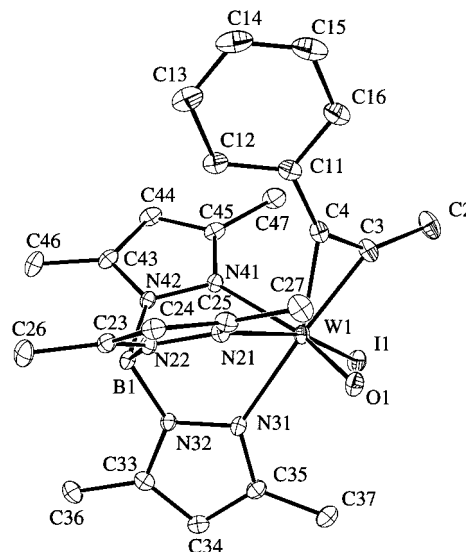


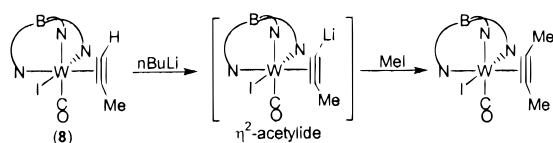
Figure 2. ORTEP diagram for Tp'W(O)(PhC≡CMe)(I) (**4**).

Table 1. Selected Bond Distances (Å) and Bond Angles (deg) for Tp'W(O)(MeC≡CH)(I) (2b)

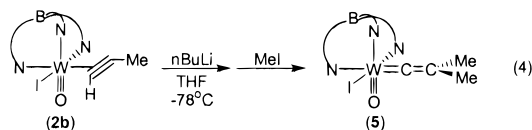
W(1)–I(1)	2.7961(5)	W(1)–N(21)	2.350(5)
W(1)–O(1)	1.712(4)	W(1)–N(31)	2.244(5)
W(1)–C(1)	2.085(6)	C(1)–C(2)	1.256(10)
W(1)–C(2)	2.117(7)	C(2)–C(3)	1.376(11)
W(1)–N(11)	2.161(5)		
I(1)–W(1)–O(1)	101.17(15)	I(1)–W(1)–C(2)	110.8(10)
I(1)–W(1)–C(1)	78.76(19)	I(1)–W(1)–N(11)	158.55(11)
I(1)–W(1)–N(21)	86.61(11)	I(1)–W(1)–N(31)	82.40(12)
O(1)–W(1)–C(1)	98.97(23)	O(1)–W(1)–C(2)	104.98(23)
O(1)–W(1)–N(11)	90.26(20)	C(1)–W(1)–N(31)	160.46(23)
O(1)–W(1)–N(21)	168.24(18)	C(2)–W(1)–N(11)	83.18(23)
O(1)–W(1)–N(31)	89.69(19)	C(2)–W(1)–N(21)	80.04(22)
C(1)–W(1)–N(11)	117.63(22)	C(2)–W(1)–N(31)	157.36(23)
C(1)–W(1)–N(21)	91.14(22)		

Table 2. Selected Bond Distances (Å) and Bond Angles (deg) for Tp'W(O)(PhC≡CMe)(I) (4)

W(1)–I(1)	2.7844(3)	W(1)–N(31)	2.244(3)
W(1)–O(1)	1.710(3)	W(1)–N(41)	2.346(3)
W(1)–C(3)	2.102(4)	C(2)–C(3)	1.488(6)
W(1)–C(4)	2.094(4)	C(3)–C(4)	1.284(5)
W(1)–N(21)	2.187(3)	C(4)–C(11)	1.465(5)
I(1)–W(1)–O(1)	101.01(9)	I(1)–W(1)–C(3)	80.29(10)
I(1)–W(1)–C(4)	112.60(9)	I(1)–W(1)–N(21)	158.46(8)
I(1)–W(1)–N(31)	82.33(7)	I(1)–W(1)–N(41)	86.35(7)
O(1)–W(1)–C(3)	97.74(14)	O(1)–W(1)–C(4)	104.91(13)
O(1)–W(1)–N(21)	88.34(12)	C(3)–W(1)–N(41)	93.15(13)
O(1)–W(1)–N(31)	90.26(12)	C(4)–W(1)–N(21)	83.06(12)
O(1)–W(1)–N(41)	167.73(12)	C(4)–W(1)–N(31)	155.52(12)
C(3)–W(1)–N(21)	117.97(12)	C(4)–W(1)–N(41)	80.84(12)
C(3)–W(1)–N(31)	161.96(12)		

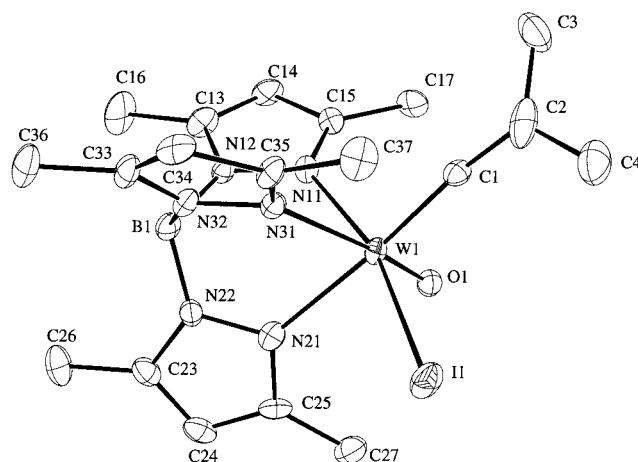
Scheme 6

product, but their chemical shifts differed from those observed in the spectrum of **3**. The absence of alkyne carbon signals in the ^{13}C NMR spectrum suggested that isomerization of the alkyne ligand had occurred. Carbon signals at 341 and 150 ppm were diagnostic of a vinylidene skeleton, and an X-ray structure confirmed this formulation (eq 4).



This result suggests that the anionic intermediate isomerizes from an η^2 - to an η^1 -acetylide prior to the addition of an electrophile (Scheme 5, path B). Significant steric interaction between the acetylide methyl group and the bulky Tp' ligand present in the η^2 -acetylide intermediate is a possible driving force for this isomerization. Additionally, the ability of the lithium cation to coordinate directly to the deprotonated carbon site during the propyne elaboration may be impeded by the large iodide ligand. Given the close proximity between the deprotonated site and the iodide ligand, the lithium cation could migrate to iodide and facilitate the η^2 to η^1 isomerization. In contrast, elaboration of the d^4 propyne complex $\text{Tp}'\text{W}(\text{CO})(\text{I})(\text{HC}\equiv\text{CMe})$ (**8**) produces an anion with less steric strain, since the methyl group is aligned along the small and cylindrical carbonyl ligand. Also, the lithium migration to iodide may not be as likely in this intermediate. The d^4 anionic intermediate can maintain η^2 coordination to produce the 2-butyne complex $\text{Tp}'\text{W}(\text{CO})(\text{MeC}\equiv\text{CMe})(\text{I})$ upon addition of MeI (Scheme 6). Attempts to directly observe the anionic intermediates in both the acetylene and propyne elaborations via low-temperature NMR using d_8 -THF were unsuccessful.

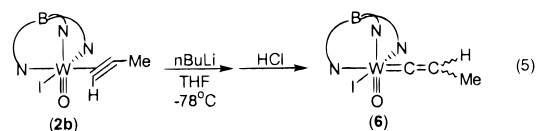
Experimental evidence of vinylidene rotation on the NMR time scale for complex **5** was sought. Heating an NMR sample of **5** in $\text{DMSO}-d_6$ showed no broadening of the vinylidene methyl resonances up to 110°C . Heating a sample of **5** to 145°C in $\text{C}_6\text{D}_5\text{Br}$ resulted in no observable broadening of the vinylidene methyl

**Figure 3.** ORTEP diagram for $\text{Tp}'\text{W}(=\text{C}=\text{CMe}_2)(\text{O})(\text{I})$ (**5**).**Table 3. Selected Bond Distances (Å) and Bond Angles (deg) for $\text{Tp}'\text{W}(=\text{C}=\text{CMe}_2)(\text{O})(\text{I})$ (**5**)**

W(1)–I(1)	2.7771(6)	W(1)–N(21)	2.282(6)
W(1)–O(1)	1.702(5)	W(1)–N(31)	2.300(6)
W(1)–C(1)	1.909(7)	C(1)–C(2)	1.345(12)
W(1)–N(11)	2.154(6)	C(2)–C(3)	1.470(16)
		C(2)–C(4)	1.534(14)
I(1)–W(1)–O(1)	98.16(16)	I(1)–W(1)–N(11)	163.10(14)
I(1)–W(1)–C(1)	91.13(21)	I(1)–W(1)–N(21)	86.52(15)
O(1)–W(1)–C(1)	98.7(3)	I(1)–W(1)–N(31)	87.43(13)
O(1)–W(1)–N(11)	93.83(21)	C(1)–W(1)–N(11)	98.8(3)
O(1)–W(1)–N(21)	89.97(22)	C(1)–W(1)–N(21)	171.2(3)
O(1)–W(1)–N(31)	169.71(20)	C(1)–W(1)–N(31)	89.74(25)

signals. Therefore, a barrier of at least 23 kcal/mol can be estimated for this tungsten(IV) d^2 vinylidene rotation. Most of the known vinylidene structures involve d^6 or d^4 metal centers and exhibit low barriers which allow for vinylidene rotation on the NMR time scale.^{11a}

Formation of a propylidene complex was accomplished by quenching the acetylide anion with excess HCl (eq 5). Complex **6** was isolated as a 1:1 mixture of isomers

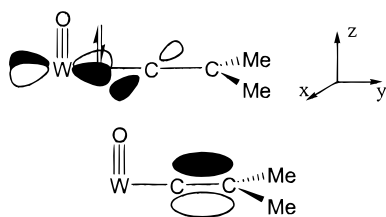


due to substituent locations at C_β with the vinylidene proton resonating as a quartet at 11.46 or at 10.79 ppm with three-bond coupling to the methyl group of 8 Hz. Doublets at 1.81 and 1.46 ppm are observed for the isomeric methyl groups. The two isomers can be distinguished by ^{13}C NMR as well, displaying C_α at 349.7 and 348.4 ppm and C_β at 138.3 and 137.5 ppm. Unfortunately, tungsten coupling to C_α is not evident; however, two-bond coupling to C_β of 40 Hz was seen.

X-ray Structure of $\text{Tp}'\text{W}(=\text{C}=\text{CMe}_2)(\text{O})(\text{I})$ (5**).** Figure 3 shows an ORTEP diagram of complex **5**. Selected bond distances and angles are given in Table 3. The $\text{W}=\text{C}_\alpha$ bond distance is 1.909(7) Å, while the $\text{C}_\alpha=\text{C}_\beta$ distance is 1.345(12) Å. Typical $\text{W}=\text{C}_\alpha$ bond lengths for group 6 vinylidenes are near 1.93 Å. The $\text{W}=\text{O}$ bond distance of 1.702(5) Å is close to the $\text{W}=\text{O}$ lengths found for alkyne complexes **2b** and **4**.

The vinylidene ligand can serve as a neutral two-electron donor and a single-faced π -acid. This formalism suggests a preferred orientation for the vinylidene

Scheme 7



fragment. Back-donation from the filled metal d_{xy} orbital to an empty p_x orbital on C_α requires formation of the C=C bond to arise from overlap of the p_z orbitals on C_α and C_β (Scheme 7). Consequently, the $C_{Me}-C_\beta-C_{Me}$ plane of the vinylidene is predicted, and shown in the structure of **5**, to be perpendicular to the W=O vector. The W=C=C fragment is nearly linear with a bond angle of 173.1° .

Conclusion

The synthesis and structure of various tungsten(IV) oxo-alkynes have been reported. The parent acetylene complex, $Tp^*W(O)(HC\equiv CH)I$, undergoes regioselective methylation to form a tungsten-propyne complex which can be elaborated to form metal-vinylidenes. Reaction of the metal-acetylene likely involves an η^2 -acetylide intermediate, while an η^2 - to η^1 -acetylide isomerization could explain vinylidene formation. While the exact driving force for this isomerization is unclear, comparisons with relevant d^4 tungsten-alkyne chemistry suggest the isomerization is possibly due to differing steric and electronic factors attributable to a change in the alkyne orientation.

Experimental Section

Materials and Methods. Reactions were performed under a dry nitrogen atmosphere using standard Schlenk techniques. Hexanes, methylene chloride, diethyl ether (Et_2O), and pentanes were purified by passage through an activated alumina column under a dry argon atmosphere. Tetrahydrofuran (THF) was distilled from sodium benzophenone ketyl under a dry nitrogen atmosphere. Methyl iodide, deuterated methylene chloride, and deuterated bromobenzene were deoxygenated using standard freeze-pump-thaw techniques and stored under a nitrogen atmosphere over 4 \AA molecular sieves.

The original synthesis of $Tp^*W(O)(CO)(I)$ involves toluene as the refluxing solvent.³ Cleaner material and higher yields were obtained using refluxing THF with an air purge for 8 h. Me_3NO , $nBuLi$ (2.5 M in hexanes), HCl (1.0 M in Et_2O), $PhC\equiv CCH_3$, $CH_3C\equiv CCH_3$, and $CH_3C\equiv CH$ were obtained and used directly from Aldrich Chemical Co. Acetylene was obtained from Matheson Gas Products Inc.

1H NMR and ^{13}C NMR spectra were recorded on a Varian XL-400 spectrometer or a Bruker WM250 spectrometer. Infrared spectra were recorded on a Mattson Polaris FT-IR spectrometer. Chemical analyses were performed by Atlantic Microlabs of Norcross, GA.

$Tp^*W(O)(I)(HC\equiv CH)$ (1). In a 500 mL round-bottom flask, $Tp^*W(O)(I)(CO)$ (3.40 g, 5.21 mmol) was dissolved in ca. 200 mL of THF. Following 10 min of purging with $HC\equiv CH$, Me_3NO (0.510 g, 6.77 mmol) was added. The reaction was stirred with a continuous $HC\equiv CH$ purge for 30 min and then for an additional 2 h under N_2 . The solvent was removed *in vacuo*. Collection of an orange fraction from an alumina column with an eluant having an increasing CH_2Cl_2 /hexanes ratio and removal of solvents gave a yellow solid. Yield: 2.10 g (62%).

IR (KBr): ν_{WO} 953 cm^{-1} . 1H NMR (CD_2Cl_2): δ 11.82, 10.49 (s, $^2J_{WH} = 13$ Hz, $HCCCH$), 6.14, 6.14, 5.61 (s, Tp^*CH), 2.89, 2.49, 2.48, 2.40, 2.32, 1.97 (s, Tp^*CH_3). ^{13}C NMR (CD_2Cl_2): δ 156.8, 145.3 ($^1J_{WC} = 30$ Hz, $^1J_{CH} = 225$ Hz, $HCCCH$), 155.6, 154.0, 152.5, 145.9, 145.9, 144.2 (Tp^*CCH_3), 108.9, 108.8, 107.9 (Tp^*CH), 18.9, 16.4, 16.2, 13.0, 12.9, 12.5 (Tp^*CH_3). Anal. Calcd for $C_{17}H_{24}BIN_6OW$: C, 31.41; H, 3.72; N, 12.93. Found: C, 31.65; H, 3.68; N, 13.00.

$Tp^*W(O)(I)(CH_3C\equiv CH)$ (2). Method A. In a 500 mL round-bottom flask, $Tp^*W(O)(I)(CO)$ (1.00 g, 1.53 mmol) was dissolved in ca. 100 mL of THF and cooled to $-78^\circ C$. Approximately 1.5 mL of $CH_3C\equiv CH$ was condensed in a graduated test tube at $-78^\circ C$. The liquid $CH_3C\equiv CH$ was transferred via cannula to the reaction mixture. Solid Me_3NO (0.148 g, 1.99 mmol) was added, and the reaction mixture was stirred for 30 min at $-78^\circ C$ and an additional 2 h at room temperature. Solvent was removed *in vacuo*. Alumina chromatography with an eluant having an increasing CH_2Cl_2 /hexanes ratio resulted in the separation of two alkyne isomers in a 1:1.5 ratio. Total yield: 0.710 g (70%). IR (KBr): ν_{WO} 943 cm^{-1} . 1H NMR (CD_2Cl_2): δ (major isomer, **2a**) 10.54 (q, $^4J_{HH} = 2.0$ Hz, $MeCCH$), 6.09, 6.09, 5.60 (s, Tp^*H), 3.79 (d, $^4J_{HH} = 3$ Hz, CH_3CCH), 2.81, 2.47, 2.45, 2.33, 2.30, 1.88 (s, Tp^*CH_3). ^{13}C NMR (CD_2Cl_2): δ 167.9 ($^1J_{WC} = 30$ Hz, $MeCCH$), 155.4, 153.8, 153.2, 145.7, 145.7, 144.2 (Tp^*CCH_3), 147.2 ($^1J_{WC} = 30$ Hz, $MeCCH$), 108.9, 108.8, 107.9 (Tp^*CH), 25.1, 19.0, 16.3, 16.1, 13.1, 12.9, 12.6 (Tp^*CH_3 and CH_3CCH). Anal. Calcd for $C_{18}H_{26}BIN_6OW$: C, 32.56; H, 3.95; N, 12.66. Found: C, 32.33; H, 3.90; N, 12.47. See method B for isomer **2b** data.

Method B. In a 250 mL round-bottom flask, **1** (0.466 g, 0.720 mmol) was dissolved in ca. 50 mL of THF and cooled to $-78^\circ C$. While the mixture was stirred, $nBuLi$ (37 μL , 0.93 mmol) was added, producing an immediate color change to give a dark purple solution. After 5 min, MeI (180 μL , 2.87 mmol) was added and the solution was stirred for 10 min at $-78^\circ C$ and then for an additional 1 h at room temperature. The solvent was removed *in vacuo*, and a dark yellow band was collected from an alumina column eluted with a solvent having an increasing CH_2Cl_2 /hexanes ratio. Recrystallization from CH_2Cl_2 /pentanes gave yellow crystals. Yield: 0.165 g (35%); two isomers in a 9:1 ratio. 1H NMR (CD_2Cl_2): δ (major isomer, **2b**) 11.76 (q, $^4J_{HH} = 3$ Hz, $MeCCH$), 6.10, 6.08, 5.60 (s, Tp^*H), 2.83, 2.46, 2.45, 2.31, 2.26, 1.94 (Tp^*CH_3), 2.29 (d, $^4J_{HH} = 3$ Hz, $MeCCH$). ^{13}C NMR (CD_2Cl_2): δ 155.4, 153.0, 151.9, 146.0, 145.7, 143.8 (Tp^*CCH_3), 154.9 ($^1J_{WC} = 30$ Hz, $^1J_{CH} = 220$ Hz, CH_3CCH), 154.6 ($^1J_{WC} = 30$ Hz, CH_3CCH), 108.7, 108.7, 107.8 (Tp^*CH), 19.0, 16.9, 16.3, 15.6, 13.0, 12.9, 12.5 (CH_3CCH and Tp^*CH_3). Anal. Calcd for $C_{18}H_{21}BIN_6OW$: C, 32.56; H, 3.95; N, 12.66. Found: C, 32.46; H, 3.92; N, 12.57.

$Tp^*W(O)(I)(MeC\equiv CMe)$ (3). In a 500 mL round-bottom flask, $Tp^*W(O)(I)(CO)$ (2.20 g, 3.37 mmol) was dissolved in ca. 200 mL of THF and cooled to $0^\circ C$. To this stirred solution, 1.0 mL of $MeC\equiv CMe$ (0.691 g, 12.8 mmol) and solid Me_3NO (0.329 g, 4.38 mmol) were added sequentially. The solution was stirred for 30 min at $0^\circ C$ and then for an additional 1 h at room temperature. Removal of solvent *in vacuo* afforded a brown-purple solid. Chromatography on alumina with an eluant having an increasing CH_2Cl_2 /hexanes ratio, solvent removal, and 2×20 mL Et_2O washes to remove a purple impurity gave a yellow solid. Yield: 1.49 g (65%). 1H NMR (CD_2Cl_2): δ 6.06, 6.05, 5.62 (s, Tp^*H), 3.62, 2.15 (q, $^4J_{HH} = 2$ Hz, CH_3CCCH_3), 2.78, 2.44, 2.44, 2.31, 2.21, 1.85 (s, Tp^*CH_3). ^{13}C NMR (CD_2Cl_2): δ 167.0, 157.7 ($^1J_{WC} = 30$ Hz, $MeC\equiv CMe$), 154.9, 152.8, 152.4, 145.7, 145.4, 143.8 (Tp^*CCH_3), 108.6, 108.5, 107.9 (Tp^*CH), 24.4, 19.0, 17.0, 16.1, 15.6, 13.0, 12.9, 12.5 (Tp^*CH_3 and CH_3CCCH_3). Anal. Calcd for $C_{19}H_{28}BIN_6OW$: C, 33.65; H, 4.16; N, 12.39. Found: C, 33.52; H, 4.15; N, 12.31.

$Tp^*W(O)(I)(PhC\equiv CMe)$ (4). To a stirred solution of $Tp^*W(O)(I)(CO)$ (1.00 g, 1.53 mmol) and $PhC\equiv CMe$ (0.535 g, 4.61 mmol) in ca. 80 mL of THF at $0^\circ C$ was added solid Me_3NO (0.140 g, 1.86 mmol). The reaction mixture was stirred for 30 min at $0^\circ C$ and then for an additional 1 h at room temperature. Solvent was removed *in vacuo*. Alumina chromatography with an eluant having an increasing CH_2Cl_2 /hexanes ratio and removal of solvents gave a yellow solid. Yield: 0.140 g (1.86 mmol). The reaction mixture was stirred for 30 min at $0^\circ C$ and then for an additional 1 h at room temperature. Solvent was removed *in vacuo*. Alumina chromatography with an eluant having an increasing CH_2Cl_2 /hexanes ratio and removal of solvents gave a yellow solid. Yield: 0.140 g (1.86 mmol).

Table 4. Crystallographic Data Collection Parameters for **2b**, **4**, and **5**

	2b	4	5
formula	C ₁₈ H ₂₄ N ₆ BIOW	C ₂₄ H ₃₀ N ₆ BIOW	C ₁₉ H ₂₈ N ₆ BIOW
mol wt	664.02	740.11	678.04
cryst syst	monoclinic	triclinic	orthorhombic
space group	<i>P2</i> ₁ / <i>c</i>	<i>P</i> $\bar{1}$	<i>Pnc2</i> ₁
<i>a</i> , Å	10.4195(5)	10.2479(4)	8.0845(4)
<i>b</i> , Å	13.1477(6)	11.5033(5)	14.0666(7)
<i>c</i> , Å	15.9428(8)	12.7961(6)	21.0611(10)
α , deg		76.6220(10)	90.0
β , deg	98.8060(10)	73.7640(10)	90.0
γ , deg		70.7860(10)	90.0
<i>V</i> , Å ³	2168.65(18)	1351.37(10)	2395.10
<i>Z</i>	4	2	4
calcd density, g/cm ³	2.034	1.819	1.880
<i>F</i> (000)	1260.55	710.32	1292.57
cryst dimens, mm	0.30 × 0.21 × 0.15	0.35 × 0.35 × 0.30	0.35 × 0.35 × 0.35
temp, °C	−100	−120	−100
radiation (λ , Å)	Mo K α (0.710 73)	Mo K α (0.710 73)	Mo K α (0.710 73)
2 θ range, deg	60.0	60.0	60.0
μ , mm ^{−1}	6.78	5.45	6.14
scan mode	ω	ω	ω
total no. of rflns	15 905	9984	17 544
total no. of unique rflns	6170	7343	5906
no. of obsd data (<i>I</i> > 2.5 σ (<i>I</i>))	5444	6782	5281
<i>R</i> _F , %	4.7	2.9	3.5
<i>R</i> _w , %	6.1	3.6	4.3
GOF	3.03	1.60	2.23

min at 0 °C and then for an additional 1 h at room temperature. Removal of solvent *in vacuo* left a brown-purple solid. Isolation of an orange band from an alumina column, removal of solvent, and recrystallization from CH₂Cl₂/pentanes produced yellow crystals. Yield: 0.510 g (45%); two isomers in a 5:1 ratio. ¹H NMR (CD₂Cl₂): δ (major isomer) 7.15 (m, 3H, *PhCCMe*), 6.44 (m, 2H, *PhCCMe*), 6.09, 5.80, 5.60 (s, *Tp'H*), 3.92 (s, *PhCCCH₃*), 2.83, 2.49, 2.48, 2.40, 1.75, 1.69 (s, *Tp'CH₃*). Selected ¹³C NMR (CD₂Cl₂): δ (major isomer) 175.0, 159.1 (¹*J*_{WC} = 35 Hz, *PhCCMe*), 155.2, 154.1, 153.2, 145.8, 144.1, 138.3 (*Tp'CCH₃*), 108.7, 108.5, 108.0 (*Tp'CH*). Anal. Calcd for C₂₄H₃₀BIOW: C, 38.95; H, 4.09; N, 11.36. Found: C, 38.92; H, 4.07; N, 11.30.

Tp'W(=C=CMe₂)(O)(I) (5). In a 250 mL round-bottom flask, *Tp'W(O)(I)(CH₃CCH)* (see method B from propyne synthesis; 0.114 g, 0.172 mmol) was dissolved in ca. 30 mL of THF and cooled to −78 °C. While the mixture was stirred, ⁿBuLi (103 μ L, 0.258 mmol) was added to give a dark green solution. Following 5 min of stirring, MeI (53 μ L, 0.121 g, 0.851 mmol) was added and the reaction mixture was warmed to room temperature. Following 45 min of stirring, solvent was removed *in vacuo*, leaving an asparagus green oil. An orange band was collected from an alumina column eluted with a solvent having an increasing ratio of CH₂Cl₂ to hexanes. Removal of solvent gave an orange solid. Yield: 0.047 g (40%). X-ray-quality crystals were formed by slow evaporative diffusion of pentanes into a CH₂Cl₂ solution of the metal complex. IR (KBr): ν_{WO} 953 cm^{−1}. ¹H NMR (CD₂Cl₂): δ 6.04, 6.04, 5.75 (s, *Tp'H*), 2.79, 2.59, 2.46, 2.45, 2.42, 2.33, 2.02, 1.54 (*Tp'CH₃* and C=C(*CH₃*)₂). ¹³C NMR (CD₂Cl₂): δ 340.8 (¹*J*_{WC} = 200 Hz, W=C=CMe₂), 154.8, 154.7, 153.5, 146.7, 145.9, 145.0 (*Tp'CCH₃*), 150.1 (²*J*_{WC} = 40 Hz, W=C=CMe₂), 108.4, 107.9, 107.6 (*Tp'CH*), 28.9, 28.2 (W=C=C(*CH₃*)₂), 18.1, 17.9, 17.7, 13.0, 12.8, 12.7 (*Tp'CH₃*). Anal. Calcd for C₁₉H₂₈BIOW: C, 33.65; H, 4.16; N, 12.39. Found: C, 33.82; H, 4.18; N, 12.20.

Tp'[C=C(H)(Me)](O)(I) (6). In a 250 mL round-bottom flask, *Tp'W(O)(I)(CH₃CCH)* (see method B from propyne

synthesis; 0.093 g, 0.140 mmol) was dissolved in ca. 25 mL of THF and cooled to −78 °C. Addition of ⁿBuLi (84 μ L, 0.210 mmol) gave a dark green solution and was followed by addition of HCl (280 μ L, 1.0 M in Et₂O, 0.280 mmol). The reaction mixture was warmed to room temperature and stirred for 45 min. Solvent was removed *in vacuo*. An orange band was collected from a silica gel column using eluant having an increasing CH₂Cl₂/hexanes ratio. Removal of solvent gave an orange solid as a 1:1 mixture of vinylidene isomers. Yield 0.035 g (38%) ¹H NMR (CD₂Cl₂): δ 11.46 and 10.79 (q, ³*J*_{HH} = 8 Hz, W=C=C(*H*)Me), 6.06, 6.06, 6.03, 5.76, 5.75 (s, *Tp'H*), 2.82, 2.80, 2.59, 2.57, 2.53, 2.51, 2.44, 2.44, 2.43, 2.41, 2.33, 2.32 (s, *Tp'CH₃*), 1.81 and 1.46 (d, ³*J*_{HH} = 7.6 Hz, W=C=C(*H*)(*CH₃*)). ¹³C NMR (CD₂Cl₂): δ 349.7 and 349.4 (W=C=C(*H*)Me), 155.1, 154.9, 154.3, 154.1, 153.6, 147.0, 146.4, 145.4, 145.2, (overlapping *Tp'CCH₃*), 138.3 and 137.5 (²*J*_{WC} = 40 Hz, W=C=C(*H*)Me), 108.6, 108.1, 107.8, 107.8 (overlapping *Tp'CH*), 25.1 and 24.3 (W=C=C(*H*)(*CH₃*)), 18.6, 18.3, 18.3, 18.2, 17.6, 13.1, 13.0, 12.9, 12.8 (overlapping *Tp'CH₃*).

X-ray Crystallography. To collect structural data, single crystals of **2b**, **4**, and **5** were each mounted on a glass wand and coated with epoxy. Diffraction data were collected on a Siemens SMART diffractometer using the ω -scan mode. The crystal of **2b** was monoclinic with space group *P2*₁/*c*. The crystal of **4** was triclinic with a space group of *P* $\bar{1}$, and the crystal studied for **5** was orthorhombic with a space group of *Pnc2*₁. Complete details are given in Table 4.

Acknowledgment. We gratefully acknowledge the National Science Foundation (Grant No. CHE-9727500) for support of this research.

Supporting Information Available: Tables giving all bond distances and angles and atomic and thermal parameters for **2b**, **4**, and **5**. This material is available free of charge via the Internet at <http://pubs.acs.org>.

OM9809926